Monatshefte für Chemie - Chemical Monthly
https://doi.org/10.1007/s00706-019-02542-z

ORIGINAL PAPER

Green synthesis of benzimidazoloquinazolines and 1,4-dihydropyridines using magnetic cyanoguanidine-modified chitosan as an efficient heterogeneous nanocatalyst under various conditions

Kaveh Javanmiri[1] · **Ramin Karimian**[1]

Received: 11 July 2019 / Accepted: 27 December 2019

Abstract

In the present study, we demonstrated the synthesis of magnetic cyanoguanidine-modified chitosan (MCGC) as an efficient and green retrievable heterogeneous nanocatalyst for one-pot three-component synthesis of benzimidazoloquinazolines (from 2-aminobenzimidazole, aromatic aldehydes, and dimedone) and 1,4-dihydropyridines (via Hantzsch-type condensation of ethyl acetoacetate, aromatic aldehydes, and ammonium acetate) under the ultrasonic irradiation and reflux conditions. The structure of the catalyst was fully confirmed using Fourier transform infrared spectroscopy, vibrating sample magnetometer, field emission scanning electron microscopy, energy dispersive spectroscopy, and thermogravimetric analysis. Increased amount of amino groups that are generated by modifying the surface of chitosan with cyanoguanidine as well as presence of hydroxyl groups determined the catalytic activity of MCGC. Furthermore, as experimental results confirmed, the ultrasonic-promoted reactions gave the better results in terms of reaction time, yield, and purity of isolated products. Cost effectiveness, mild conditions, low catalyst loading, convenient work-up, and ecofriendly solvent are some of the remarkable advantages of this protocol.

Graphic abstract

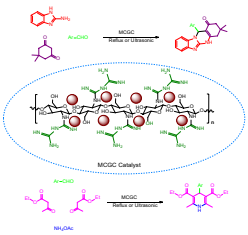

Keywords Chitosan · Ultrasonic irradiation · Benzimidazoloquinazolines · 1,4-Dihydropyridines · Magnetic nanocatalyst · Cyanoguanidine

Introduction

The use of homogeneous catalysts is restricted by two important factors, high cost of materials and tedious separation procedures. In this respect, the recovery of homogeneous catalysts by filtration or centrifugation involves tedious work-up as well as these procedures result in the remarkable loss amount of nanocatalyst. As an ideal choice, the development of magnetically separable nanocatalysts has

Electronic supplementary material The online version of this article (https://doi.org/10.1007/s00706-019-02542-z) contains supplementary material, which is available to authorized users.

✉ Ramin Karimian
Karimian.r@gmail.com

[1] Chemical Injuries Research Center, Systems Biology and Poisonings Institute, Baqiyatallah University of Medical Sciences, Tehran, Iran

Published online: 28 January 2020

been emerged as an effective technique [1]. Recently, the magnetic catalysts have been utilized in various organic transformations [2–4]. "Green Chemistry" rules, monitor the design of chemicals and processes to decrease or eliminate the use and production of hazardous substances [5]. The application of biopolymers such as starch [6], cellulose [7], chitosan [8], and wool [9] as a support in heterogeneous catalysis is an emerging field. Of these, chitosan is especially demanding because it is a non-toxic, hydrophilic, biocompatible, biodegradable, and antibacterial bifunctional biopolymer. Chitosan directly promotes several organic reactions such as transamidation [10], Strecker reaction [11], Biginelli reaction [12], Ullmann reaction [13], aldol and Knoevenagel reactions [14, 15], and pyridazine synthesis [16] owing to the existence of $–NH_2$ and –OH groups on its surface. In fact, chitosan serves as an organocatalyst and promotes the green and metal-free processes. In addition, chitosan plays an important role as a support for metals to catalyze several reactions such as Suzuki-Miyaura and Heck cross-coupling reactions [17, 18], oxidation [19, 20], and [3+2] Huisgen cycloaddition [21]. Besides, chitosan is used in food packing, adhesives, medicine, drug delivery, agriculture, membrane, treatment, and fuel cells [22]. By modifying the surface of chitosan with organic molecules, new properties appear in the modified chitosan. Various techniques for modification of chitosan have been reported [23]. For example, Kumar and co-workers described a diisocyanate-modified chitosan with antibacterial activity against *E. coli* [24]. In the field of catalyst, Dekamin et al. reported a melamine-modified chitosan materials as an organocatalyst for the synthesis of dihydropyrano[2,3-*c*]pyrazole and benzylpyrazolyl coumarin derivatives. Guanidinylation of chitosan increases the amount of the amino groups on the chitosan as reported by independent groups [25, 26]. Multicomponent reactions (MCRs) demonstrate superior atom economy and efficiency as compared to the classical methods for the synthesis of complex molecules. Therefore, the improvement of new multicomponent reactions (MCRs) and the progression of known MCRs are utmost important in medicinal and organic chemistry [27–29]. MCRs pave the synthesis of desired structures from three or more than three starting materials [30, 31]. The reactions under the ultrasonic irradiation benefit from various advantages in the terms of reaction rates, yields, purity of the products, selectivity, short reaction times, and milder conditions, and etc. [32–34]. In the ultrasound-assisted reactions a huge number of cavitation bubbles are generated and their collapsing forms micro-jets that provide fine emulsion between substrates [35]. Due to their potent physiological properties, nitrogen-containing heterocycles play a vital role in the pharmaceutical and agrochemical industries [36]. Of these, quinazolinone derivatives display a wide range of pharmacological and biological activities such as antihypertensive [37], antihistaminic [38], analgesic and anti-inflammatory [39], anticancer [40], and anti-HIV [41], etc. In addition, quinazolines exist in the structure of many natural products, ligands, and C−H bond activation partners [42, 43]. Benzimidazoles are common pharmacophores in the modern drug design due to their presence in natural products and biologically active molecules [44]. Benzimidazoles are reported as bactericides and anti-carcinogens [45–47]. Benzimidazoloquinazolines incorporate both benzimidazole and quinazole moieties. Intrigued by their importance, many methods have been reported by independent groups [48–50]. Recently, Singh et al. developed a method for the synthesis of benzimidazolo/benzothiazolo quinazolinone derivatives using $Sc(OTf)_3$ under the microwave irradiation [51]. As one of the most frequented MCRs, Hantzsch reaction has attracted much attention in the synthesis of 1,4 dihydropyridines (1,4-DHPs) due to their remarkable biological activities and pharmacological properties [52, 53]. 1,4-DHPs are used as anticonvulsant, antidiabetic, antianxiety, antidepressive, antitumor, radio- and neuroprotectant platelet anti-aggregratory [54–57]. Besides, 1,4-DHPs are also useful as reducing agents for imines in the presence of a catalytic amount of Lewis acid [58]. 1,4-DHPs are generally prepared by the classical Hantzsch method, which is a cyclocondensation reaction of aldehyde, *β*-ketoesters, and ammonia either in acetic acid or in refluxing ethanol that suffers from long reaction times and low yields [59]. Several methods have been reported to modify this reaction by various catalyst such as *p*-TSA [60], cellulose sulfuric acid [61], L-proline [62], chitosan-supported copper(II) sulfate (CSCS) [63], aminated multi-walled carbon nanotubes [64], silica-supported ceric ammonium nitrate (CAN) [65], nicotinic acid [66], sulfated polyborate [67], benzyltrimethylammonium fluoride hydrate, and supported chitosan [68]. Although the described methods are effective, however, these protocols are associated with remarkable disadvantages such as hazardous solvents, toxic reagents, prolonged reaction time, high temperature, use of toxic metals, strongly acidic condition, and sometimes loss of recyclability of the catalyst. To pave these disadvantages, in this paper, we would like to demonstrate a magnetic cyanoguanidine-modified chitosan (MCGC) as an efficient heterogeneous magnetic organocatalyst for the synthesis of benzimidazoloquinazoline and 1,4-DHPs under reflux and ultrasonic-assisted conditions (Scheme 1). Benzimidazoloquinazoline derivatives **5** were prepared via a one-pot three-component condensation reaction starting from 2-aminobenzimidazole (**2**), aromatic aldehydes **3a**–**3h**, and dimedone (**4**) under ultrasonic-assisted conditions. Additionally, 1,4-DHPs were produced through a multicomponent reaction using 2 eq. ethyl acetoacetate (**6**), 1 eq. of aromatic aldehydes **3a**-**3h'**, and 1 eq. ammonium acetate (**7**).

Scheme 1

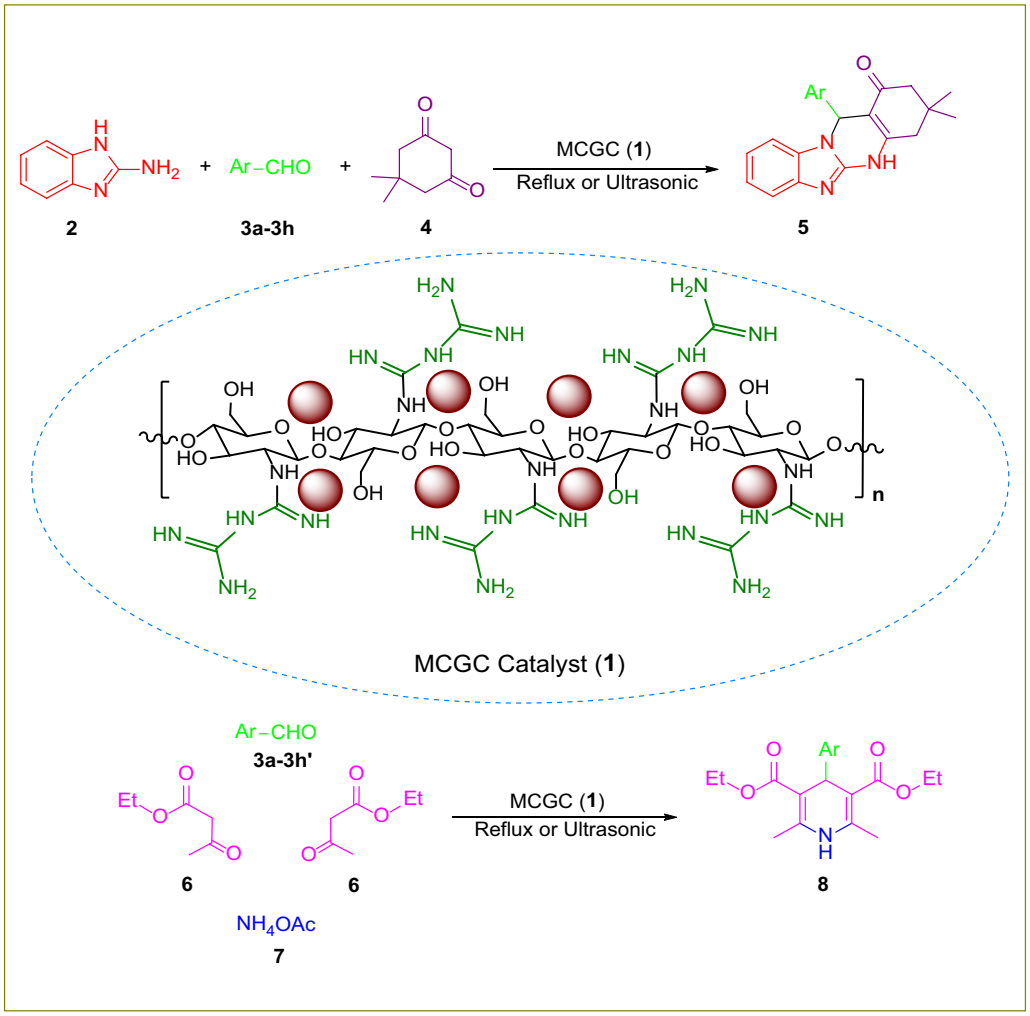

Results and discussion

Catalyst preparation

General description for the preparation of MCGC catalyst (**1**) from commercial chitosan is shown in the Scheme 2. Firstly, chitosan was modified by cyanoguanidine in the 37% HCl solution to produce CGC. Next, stirring the CGC with a mixture of $FeCl_3{\cdot}6H_2O$ and $FeCl_2{\cdot}4H_2O$ dissolved in deionized water and then addition of aqueous 25% aqueous ammonia followed by washing and drying afforded magnetic cyanoguanidine-modified chitosan (MCGC, **1**).

Catalyst characterization

The synthesized nanocatalyst **1** was characterized using different physicochemical techniques such as Fourier transform infrared spectroscopy (FT-IR), vibrating sample magnetometer (VSM), field emission scanning electron microscopy (FESEM), energy dispersive spectroscopy (EDX), and thermogravimetric analysis (TGA). The FT-IR spectroscopy analysis was performed to confirm the structure of chitosan (a), CGC (b), MCGC (c), and recycled MCGC (d) by identifying the desired functional groups as shown in Fig. 1. In the FT-IR spectrum of chitosan (a), the absorption band at 3442 cm^{-1} is ascribed to the vibrational stretching of the N–H and O–H groups with an overlapping. The stretching vibration of aliphatic C–H groups appeared at 2910 cm^{-1}. Furthermore, the stretching vibrations of C–O–C bond is located at 1100 cm^{-1}. After modification of chitosan with cyanoguanidine a new band appeared at 1645 cm^{-1} which is assigned to functional groups of CGC [69]. In the FT-IR spectrum of MCGC a new adsorption peak appeared at 592 cm^{-1} which corresponds to the Fe–O that indicates the presence of FeO linkages in ferric oxide.

To understand the composition and distribution of individual components in the chitosan and MCGC (**1**) nanocomposites, we performed energy-dispersive X-ray spectroscopy (EDX) and elemental mapping at different parts of the specimens. The results are depicted in Fig. 2a, b and c.

Scheme 2

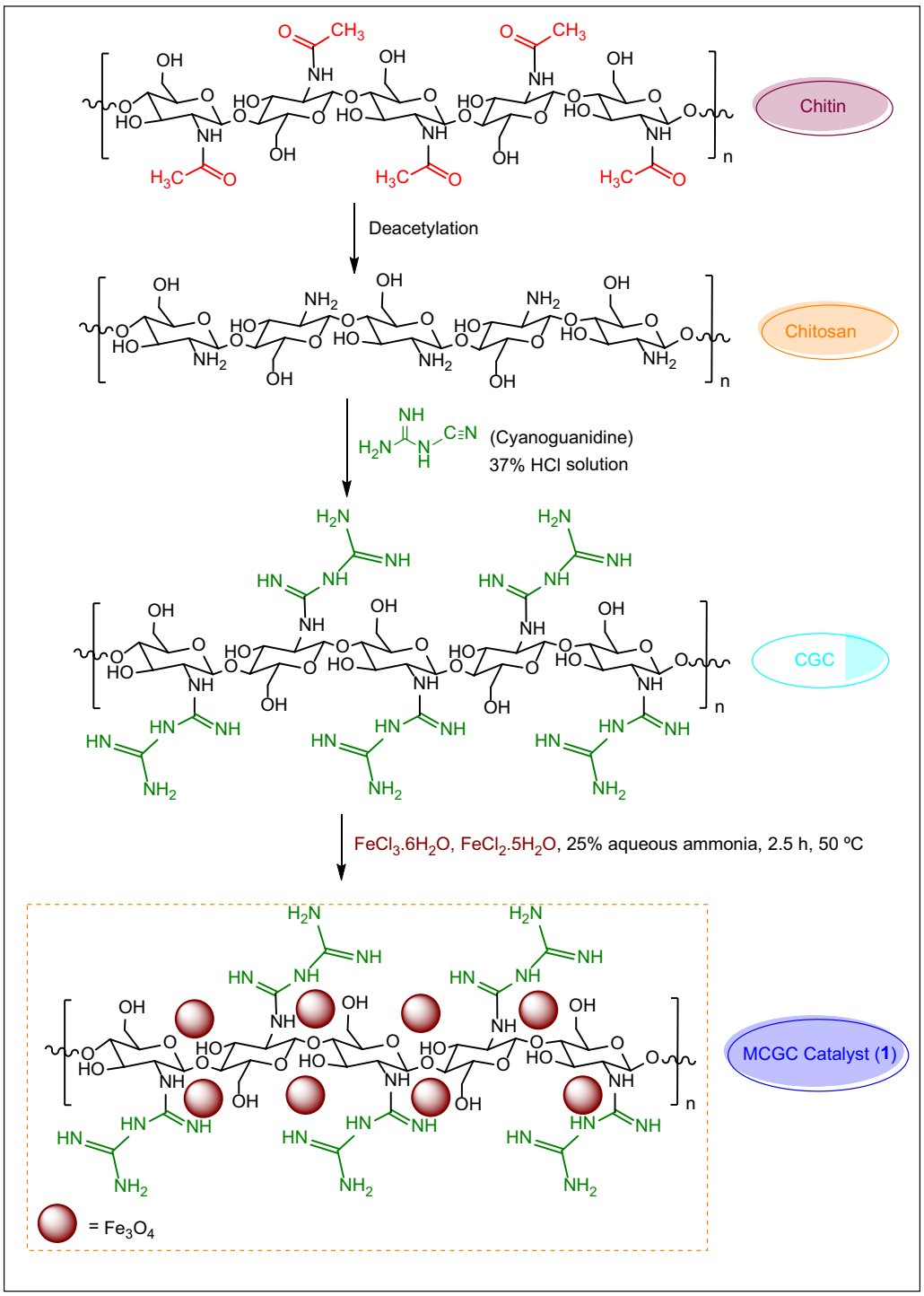

To investigate the particle size, surface shape and the morphology of MCGC (**1**), we performed the FESEM analysis. As it can be seen from the FESEM micrograph of MCGC (**1**), the nanocomposite was made up of almost spheroidal nanoparticles. The majority of the nanoparticles were in the range of 28-33 nm particle size (Fig. 3). Additionally, the Fe_3O_4 nanoparticles are properly loaded on the surface of CGC. Magnetization behavior of the Fe_3O_4 and MCGC (**1**) nanoparticles under the applied magnetic field at room temperature has been depicted in Fig. 4. The values of the magnetization saturation (M_s) for Fe_3O_4 and MCGC (**1**) were 80.08 and 47.85 emu/g, respectively. The lower M_s for MCGC (**1**) compared with Fe_3O_4 may be due to the larger size of particles in MCGC (**1**).

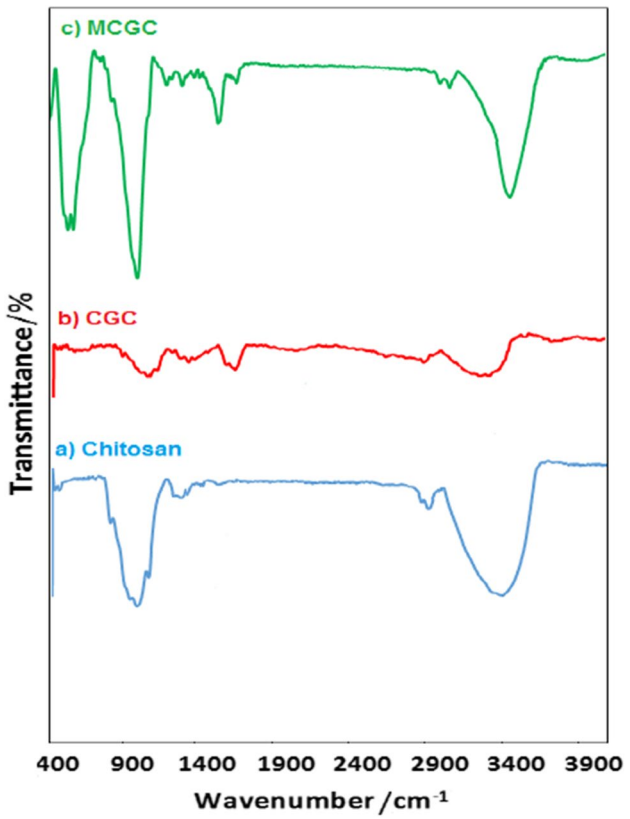

Fig. 1 FT-IR spectra of chitosan (**a**), cyanoguanidine-modified chitosan (CGC) (**b**), and magnetic cyanoguanidine-modified chitosan (MCGC) (**c**)

The thermal stability of MCGC (**1**) was analyzed by thermogravimetric analysis (TGA). The initial weight loss before 100 °C is related to the removal of the adsorbed water and surface hydroxyl groups of the Fe_3O_4 nanoparticles. Figure 5 represents the TG curve of MCGC (**1**) catalyst under the nitrogen atmosphere over 20–800 °C. The weight loss in the range of 220–750 °C was ascribed to the decomposition of organic moieties (chitosan and cyanoguanidine). Total weight loss of the MCGC (**1**) was around 40% until 800 °C.

Application of MCGC as an efficient nanocatalyst for the synthesis of benzimidazoloquinazolines and 1,4-DHPs

The catalytic activity of MCGC (**1**) was initially investigated in a standard reaction using 2-aminobenzimidazole (**2**, 1 mmol), benzaldehyde (**3g**, 1 mmol) and dimedone (**4**, 1 mmol) for the synthesis of benzimidazoloquinazoline derivatives and benzaldehyde (**3g**, 1 mmol), ethyl acetoacetate (**6**, 2 mmol) and ammonium acetate (**7**, 1 mmol) for the synthesis of 1,4-DHPs. The effect of the solvent, temperature, amount of the catalyst, and irradiation frequency was explored to establish the general reaction conditions. The results are summarized in Table 1. First, a reaction was carried out in the absence of catalyst and solvent (Table 1, entry 1) that only a trace amount of desired product (**5g** and **8g**) was resulted. Besides, an improvement in the yield of reaction was observed by using 5 mg of MCGC (**1**) in CH_3CN as solvent (Table 1, entry 2). In the next step, to evaluate the effect of ultrasonic irradiation equivalent reactions were carried out with 5 mg of MCGC (**1**) in the various solvents such as CH_3CN, H_2O, MeOH, EtOH:H_2O, and EtOH under the ultrasonic irritation (25 kHz frequency) at 20–22 °C for 30 min (Table 1, entries 3–7). As shown (Table 1, entry 7), the best result was obtained in EtOH as the solvent for benzimidazoloquinazolines and 1,4-DHPs because of its benign nature, better homogenity of substrates, low cost and wide availability as compared with other organic solvents, although the reaction could even be successfully accomplished in the protic solvents like MeOH and H_2O or EtOH:H_2O.

With 15 mg of catalyst loading, the yield of the products **5g** and **8g** were increased to 89% and 85% respectively (Table 1, entry 9). The reaction temperature also has an appreciable influence on the reaction yield under the ultrasound irradiation. Therefore, we increased the temprerature to 30–32 °C and surprisingly the reaction yield improved (Table 1, entry 10).

Unlike to 1,4-DHPs, in the case of benzimidazoloquinazolines no significant improvement in the reaction yield was observed by increasing the temperature to 40–42 °C (Table 1, entry 12). In addition, the reaction with 40 kHz ultrasound irradiation also afforded the same reaction yield that showed the frequency of irradiation had not remarkable influence on the yield of both reactions.

According to the above results, the optimized reaction conditions for the synthesis of benzimidazoloquinazolines was determined as: 2-aminobenzimidazole (**2**, 1 mmol), aromatic aldehyde (**3f**, 1 mmol), dimedone (**4**, 1 mmol), EtOH as solvent (5 cm^3), MCGC (**1**, 15 mg), bath temperature 40–42 °C, and irradiation frequency 25 kHz (Table 1, entry 10). The optimized reaction condition for the synthesis of 1,4-DHPs was determined as: aromatic aldehyde (**3**, 1 mmol), ethyl acetoacetate (**6**, 2 mmol) ammonium acetate (**7**, 1 mmol) aromatic aldehydes (1 mmol), MCGC (**1**, 15 mg), ethanol (5 cm^3) bath temperature 30–32 °C, and irradiation frequency 25 kHz (Table 1, entry 11).

With the optimal reaction conditions in hand, we investigated the scope and generality of this protocol for the preparation of benzimidazoloquinazolines and 1,4-DHPs. The results shown in Table 2 confirmed the compatibility of this methodology with a broad range of aromatic aldehydes (**3a**–**3h**) bearing electron donating and electron withdrawing groups on the benzene ring.

All experiments reported in Table 2 were carried out under the ultrasonic irradiation and in the reflux conditions.

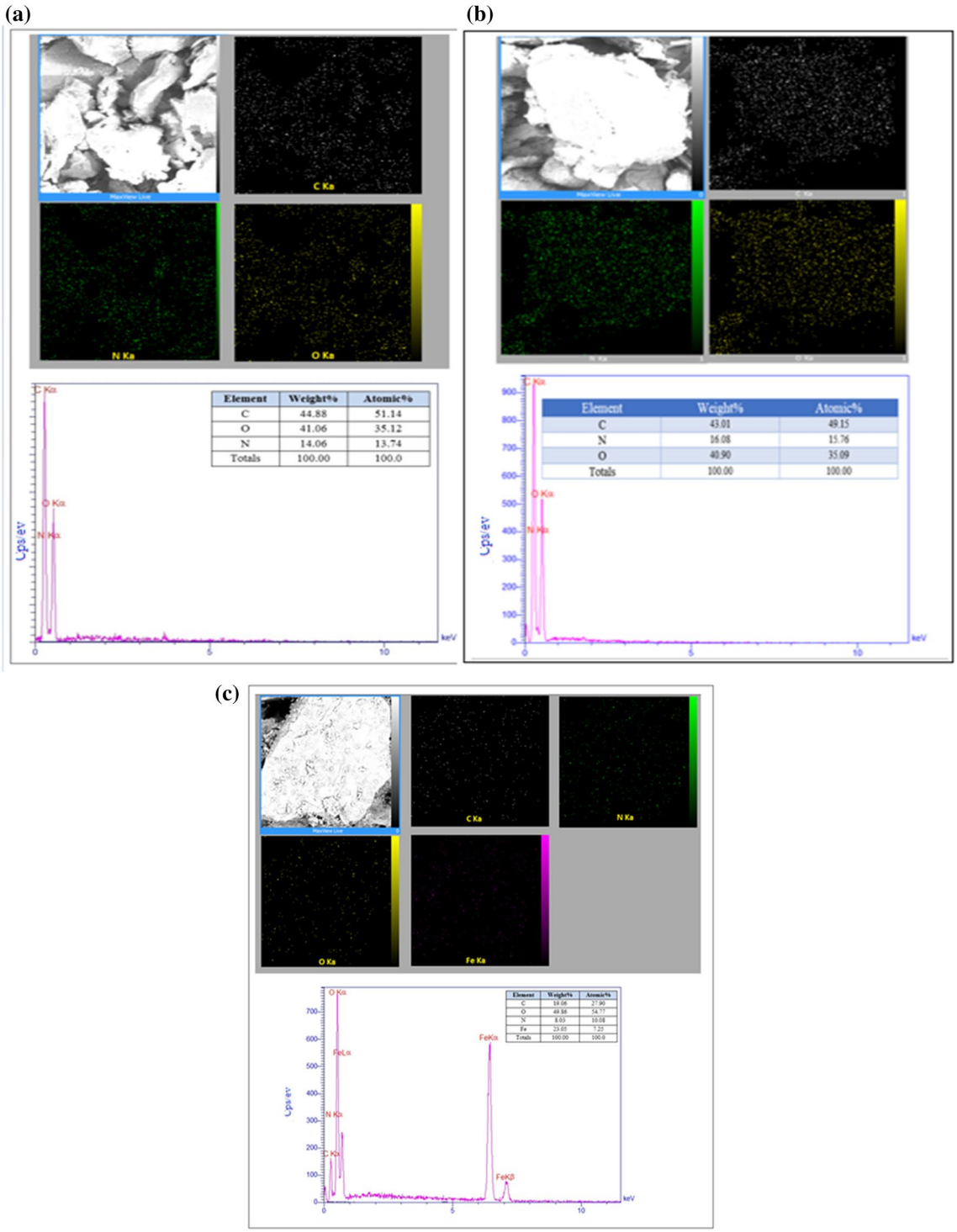

Fig. 2 EDX spectra and elemental mapping of chitosan (**a**), CGC (**b**), and MCGC (**c**) nanoparticle

The advantages of ultrasonic irradiation were the shorter reaction times, high yield and remarkable purity of products comparing with condensation in the refluxing ethanol. For example, the synthesis of **5a** and **5b** in the refluxing ethanol needed 80 min and 90 min to obtain 87% and 85% yield, respectively. Whereas, the same experiment by applying ultrasonic irradiation at 30–32 °C resulted **5a** and **5b** within 35 min and 40 min with 95% and 92% yield respectively.

These results indicated that, to prepare the benzimidazoloquinazoline derivatives (Table 2, entries 1–8) and

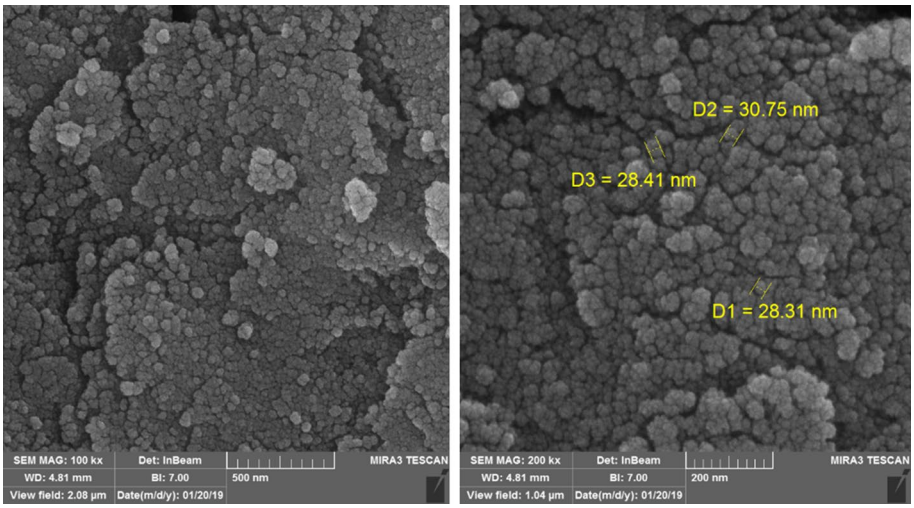

Fig. 3 FESEM micrograph of MCGC (**1**)

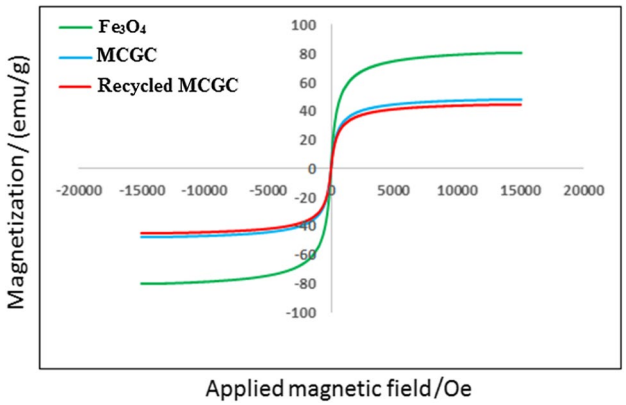

Fig. 4 Magnetization curves of Fe_3O_4, fresh MCGC and recovered MCGC after run 8 at room temperature

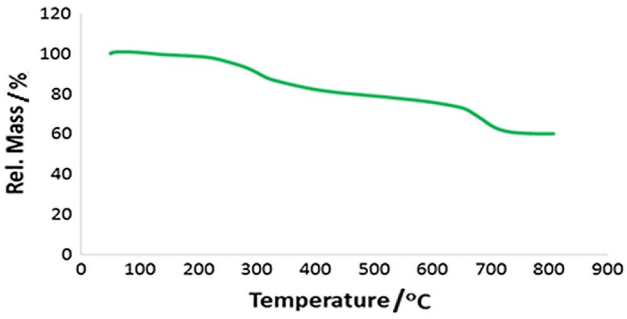

Fig. 5 The TGA curve of MCGC (**1**) nanoparticles

1,4-DHPs using MCGC (**1**) nanocatalyst, the ultrasonic irradiation is a superior method as compared to the reflux conditions [75].

Proposed reaction mechanism for the synthesis of benzimidazoloquinazoline derivatives **5a**–**5h** based on the available literature [48–50, 76] is depicted in Scheme 3. Presence of hydroxyl and amino groups appears bifunctional characteristics in the MCGC (**1**) catalyst. Initially, a Knoevenagel condensation between activated aldehyde **3a**-**3h** and dimedone (**4**) produces the intermediate **A**. In the next step, activation of carbonyl group on the intermediate (**A**) facilitates the attack of 2-aminobenzimidazole (**2**) to intermediate **A** that results in intermediate **B**. Next, intermediate **B** converts to intermediate **C** upon releasing the water molecule. Finally, cyclization of intermediate **C** leads to the corresponding benzimidazoloquinazoline **5a**–**5h**. A plausible reaction mechanism for the preparation of 1,4-DHPs using MCGC (**1**) catalyst is presented in Scheme 4. In the first step, 1 equiv. of ethyl acetoacetate (**6**) is converted into its enol form by MCGC (**1**), which affords nucleophilic addition to the activated carbonyl groups **3a**–**3h'** to form Knoevenagel product **A'**. Next step involves the formation of β-enaminoester **B'** from the second equiv. of ethyl acetoacetate (**6**) and in-situ produced ammonia from ammonium acetate (**7**). After that, Michael addition between **B'** and **A'** generates **C'** which is converted to the corresponding 1,4-DHP **8a**–**8h'** through a cyclization and elimination of H_2O.

The efficiency of present protocol was compared with some of recently reported methods for the synthesis of benzimidazoloquinazolines **5a**–**5h** and 1,4-DHPs **8a**–**8h'**. The results are collected in Table 3 for **5g** and **8g** as model substrates. As it can be seen, this method is superior to some of these methods in terms of catalyst loading, solvent, temperature, reaction time, and yield.

For a heterogeneous catalyst ease of separation and reusability are two important factors. The reusability of MCGC (**1**) was evaluated for **5g** and **8g** as model substrates. After the completion of each reaction an external magnet was used to separate the MCGC (**1**). Then, the catalyst was washed with water (3×10 cm^3) and ethanol (1×10 cm^3) and finally, dried in an oven at 50 °C for 1 h. The efficiency

Table 1 Optimization of reaction conditions for the preparation of benzimidazoloquinazolines[a] and 1,4-DHP[b] derivatives in a model reaction

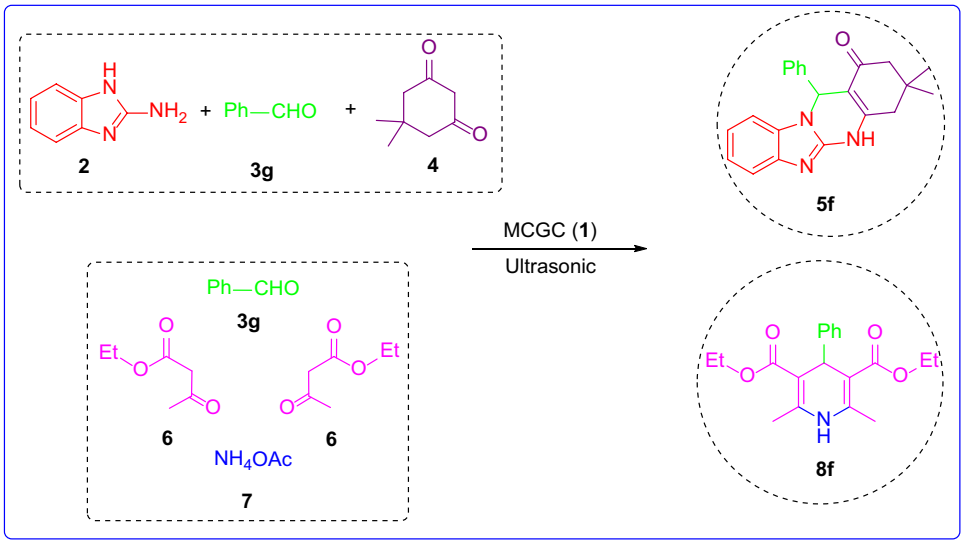

Conditions				Benzimidazoloquinazolines		1,4-DHPs	
Entry	Catalyst/mg	Solvent	Temp./°C	Time/min	Yield[c]/%	Time/in	Yield[c]/%
1	–	–	–	30	Trace	15	Trace
2	5	CH_3CN	r.t.	30	30	15	20
3	5	CH_3CN	20–22	30	40	15	25
4	5	H_2O	20–22	30	35	15	30
5	5	MeOH	20–22	30	55	15	55
6	5	EtOH-H_2O	20–22	30	45	15	50
7	5	EtOH	20–22	30	65	15	60
8	10	EtOH	20–22	30	77	15	76
9	15	EtOH	20–22	30	89	15	85
10	15	EtOH	30–32	30	93	15	92
11	15	EtOH	40–42	30	93	15	95
12[d]	20	EtOH	40–42	30	93	15	95

[a]Reaction conditions: 2-aminobenzoimidazole (**2**, 1 mmol), benzaldehyde (**3g**, 1 mmol), dimedone (**4**, 1 mmol) in the presence of MCGC (**1**), 5 cm^3 of each solvent, and irradiation frequency of 25 kHz

[b]Reaction conditions: benzaldehyde (**3g**, 1 mmol), ethyl acetoacetate (**6**, 2 mmol), ammonium acetate (**7**, 1 mmol) in the presence of MCGC (**1**), 5 cm^3 of each solvent, and irradiation frequency of 25 kHz

[c]Isolated yields

[d]Irradiation frequency of 40 kHz

of the recycled catalyst was examined up to eight consecutive runs and its catalytic efficiency remained almost the same (Fig. 6).

Figure 7 depicts the FT-IR spectrum of fresh MCGC (a) and recycled MCGC (b) after run 8th. As it can be seen, the FT-IR of recycled MCGC (b) is similar to the fresh MCGC (a) with a decrement in the intensity of some peaks that confirms the stability of MCGC. In addition, magnetic properties of the recycled MCGC after the 8th run (Fig. 4) showed a very slight decrease in the M_s value (Fig. 4) that could be attributed to leaching of Fe_3O_4 nanoparticles from surface of CGC. This fact also was confirmed by ICP-OES analysis in which the results showed a decrement in the concentration of Fe from 42.885 wt% for fresh MCGC to 41.335 wt% for recovered MCGC after 8th run.

Table 2 One-pot synthesis of benzimidazoloquinazolinone derivatives[a] and 1,4-DHPs[b] using MCGC (**1**) nanocatalyst

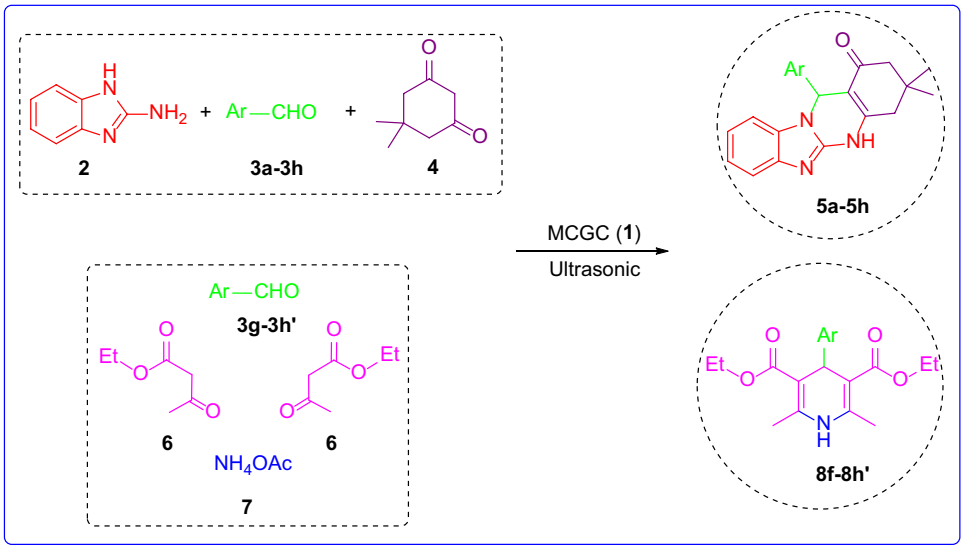

Entry	Ar	Product	Ultrasonic irradiation		Reflux		M.p. /°C Obs. (Lit.)
			Time/min	Yield/%[c]	Time/min	Yield/%[c]	
1	4-Cl-C_6H_4 (**3a**)	**5a**	35	95	80	87	330–333 (336–339 [70])
2	2-Cl-C_6H_4 (**3b**)	**5b**	40	92	90	85	352–354 (352–355 [70])
3	4-NO_2-C_6H_4 (**3c**)	**5c**	37	96	83	91	> 360 (374–378 [71])
4	3-NO_2-C_6H_4 (**3d**)	**5d**	33	91	77	87	340–342 (338–340 [51])
5	4-CH_3-C_6H_4 (**3e**)	**5e**	55	90	95	86	325–327 (325–328 [72])
6	4-OH-C_6H_4 (**3f**)	**5f**	66	91	85	88	331–333 (> 300 [70])
7	C_6H_5 (**3g**)	**5g**	30	93	75	90	307–309 (308–310 [73])
8	4-Pyridinyl (**3h**)	**5h**	14	89	48	84	297 (298–300 [74])
9	4-Cl-C_6H_4 (**3a**)	**8a**	12	96	15	89	142–144 (144–146 [26])
10	2-Cl-C_6H_4 (**3b**)	**8b**	15	92	17	87	126–128 (127–128 [26])
11	4-NO_2-C_6H_4 (**3c**)	**8c**	10	94	15	89	130–132 (127–129 [67])
12	3-NO_2-C_6H_4 (**3d**)	**8d**	12	93	16	86	163–165 (163–164 [67])
13	4-CH_3-C_6H_4 (**3e**)	**8e**	16	90	24	85	133–135 (134–135 [67])
14	4-OH-C_6H_4 (**3f**)	**8f**	18	92	27	86	229–231 (230–231 [67])
15	C_6H_5 (**3g**)	**8g**	15	95	17	92	156–158 (157–158 [67])
16	2-Furyl (**3h'**)	**8h'**	12	94	17	89	165–166 (164–167 [69])

[a]Ultrasonic irradiation: 2-aminobenzoimidazole (**2**, 1 mmol), aldehyde **3a–3h** (1 mmol), dimedone (**4**, 1 mmol), MCGC (**1,** 15 mg), 5 cm^3 EtOH, irradiation frequency of 25 kHz and 30–32 °C temperature. Reflux conditions: 2-aminobenzoimidazole (**2**, 1 mmol), aldehyde **3a–3h** (1 mmol), dimedone (**4**, 1 mmol) and MCGC (**1,** 15 mg) in 5 cm^3 refluxing EtOH

[b]Ultrasonic irradiation: aldehyde **3a-3h'** (1 mmol), ethyl acetoacetate (**6**, 2 mmol), ammonium acetate (**7**, 1 mmol), MCGC (**1,** 15 mg), 5 cm^3 EtOH, irradiation frequency of 25 kHz and 40–42 °C temperature. Reflux conditions: aldehyde **3a–3h'** (1 mmol), ethyl acetoacetate (**6**, 2 mmol), ammonium acetate (**7**, 1 mmol) and MCGC (**1,** 15 mg) in 5 cm^3 refluxing EtOH

[c]Isolated yields

Conclusion

In conclusion, we have found magnetic cyanoguanidine-modified chitosan (MCGC) as an efficient and reusable magnetic nanocatalyst for one-pot three-component synthesis of benzimidazoloqunazolines (from 2-aminobenzimidazole, aromatic aldehydes, and dimedone) and 1,4-DHPs (via Hantzsch-type condensation of ethyl acetoacetate, aromatic aldehydes, and ammonium acetate)

Scheme 3

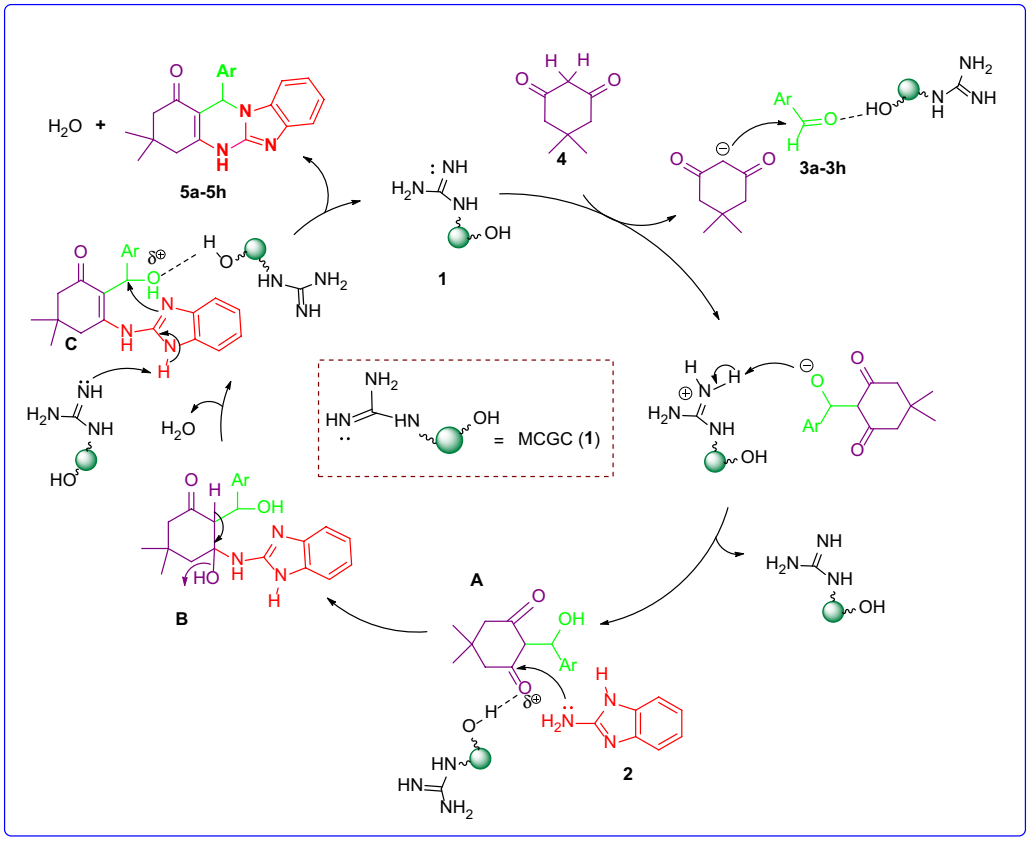

under the ultrasonic irradiation and reflux conditions. The results confirmed that the ultrasonic irradiation is a superior method as compared to the reflux conditions. Ease of work-up procedures, mild conditions, short reaction times, high yields, reusable catalyst, low catalyst loading, and compatibility with a broad range of aromatic aldehydes are some of precious advantages of the described method.

Experimental

All chemicals were procured from Merck or Aldrich companies and used without further purifications. Commercial chitosan (MW = 6,00,000–8,00,000 Dalton) was procured from Acros Organics. Moreover, the products were characterized by comparison of their spectral data and physical properties with those reported in the literature. The reaction progress was monitored by TLC using Merck 0.2 mm silica gel 60F-254 Al-plates. FT-IR spectra were obtained as KBr pellets on a Shimadzu FTIR-8400S spectrometer in the range of 4000-400 cm^{-1}. ^1H NMR spectra were recorded on a Bruker DRX 300 MHz Avance spectrometer in $CDCl_3$ or DMSO-d_6 as solvent at ambient temperature. Melting point of products were determined in open capillaries with a Electrothermal IA9100 melting point apparatus. The surface morphology, size, and shape of the catalyst was evaluated by field emission scanning electron microscopy (FESEM, MIRA3, TESCAN, Czech Republic). Energy dispersive spectroscopy (EDX) patterns were obtained using MIRA III instrument of TESCAN Company, Czech Republic to identify the chemical elements. The concentration of Fe was assessed using Shimadzu AA-680 flame atomic absorption spectrophotometer and inductively coupled plasma optical emission spectrometer (ICP-OES) Varian Vista PRO Radial. The crystal structure of MCGC (**1**) was analysed on an X'Pert MPD Philips diffractometer with Cu radiation source (λ = 1.54050 Å) at 40 kV voltage and 40 mA current. The magnetic properties of MCGC (**1**) were analysed using vibrating sample magnetometer (VSM, BHV-55, Riken, Japan) at room temperature. Thermal stability of desired MCGC (**1**) was determined by thermogravimetric analysis (TGA) using Bahr company STA 504 instrument. Ultrasonic irradiation was performed by using a Shanghai Branson-BUG25-06 ultrasonic cleaner with a frequency of 25 or 40 kHz.

Scheme 4

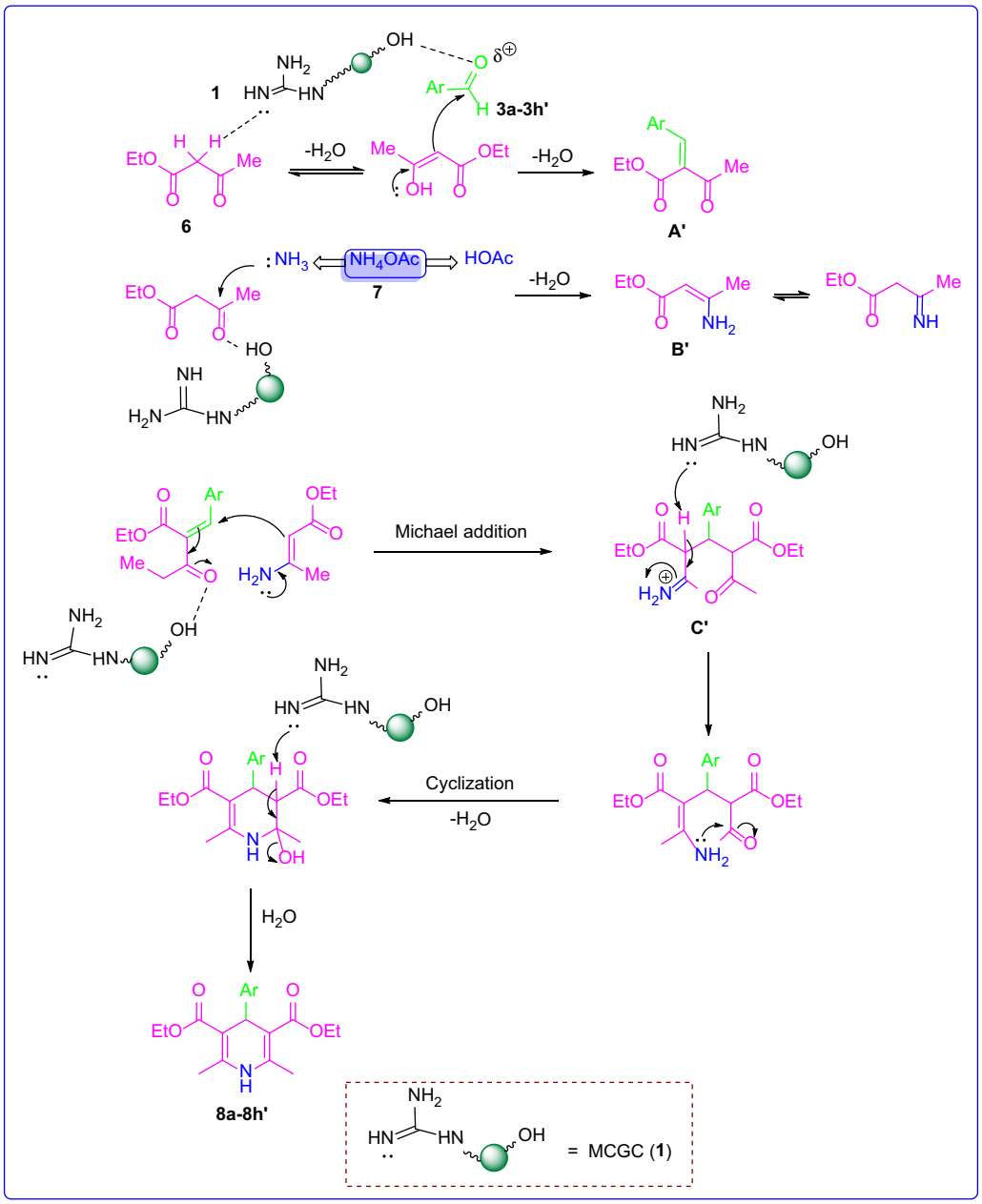

Preparation of cyanoguanidine-modified chitosan (CGC)

First, 0.5 g chitosan was dissolved in 30 cm^3 of 37% HCl solution and stirred for 30 min at room temperature. Then, 2.0 g cyanoguanidine was added to the premixed solution and the obtained mixture was stirred at 60 °C for 24 h. After that, a solution of NaOH in distilled water (0.5 M) was slowly added to the mixture to obtain a clear precipitate. The obtained precipitate was thoroughly washed with distilled water and ethanol to remove unreacted materials and then dried in an oven at 80 °C for 12 h.

Preparation of magnetic cyanoguanidine-modified chitosan (MCGC)

Briefly, 1.56 g $FeCl_3{\cdot}6H_2O$ (0.0057 mol) and 0.76 g $FeCl_2{\cdot}4H_2O$ (0.0038 mol) were dissolved in 40 cm^3 water and stirred for 10 min. Then, 0.5 g CGC was added to the premixed solution and after addition of 10 cm^3 of 25% aqueous ammonia during 30 min the mixture was stirred for 2.5 h at 50 °C. Finally, the obtained MCGC (**1**) was separated from the solution using an external magnet, thoroughly washed with distilled water and ethanol and dried in an oven at 60 °C for 24 h.

Table 3 Comparative synthesis of compounds **5g** and **8g** with reported methods compared with the present method

Entry	Catalyst	Catalyst loading	Solvent	Temp/°C	Time/min	Yield/%	Product	References
1	NH_2SO_3H	5 mg	CH_3CN	Reflux	15	94	**5g**	[50]
2	Fe_3O_4@IM	30 mg	EtOH	78	40	87	**5g**	[70]
3	Fe_3O_4@GO	65 mg	EtOH	Reflux	35	91	**5g**	[77]
4	Nano-WO_3-SO_3H	19 mg	Solvent-free	100	15	94	**5g**	[78]
5	MCGC (**1**)/Ultrasonic	15 mg	EtOH	30–32	30	93	**5g**	–
6	MGCS	30 mg	EtOH	Reflux	15	89	**8g**	[26]
7	Aminated MWCNTs	1 mg	EtOH	Reflux	240	85	**8g**	[64]
8	Nicotinic acid	0.1 g	Solvent-free	80	5	95	**8g**	[66]
9	ChVO	5 mg	Solvent-free	85	55	89	**8g**	[69]
10	MCGC (**1**)/Ultrasonic	15	EtOH	40–42	15	95	**8g**	–

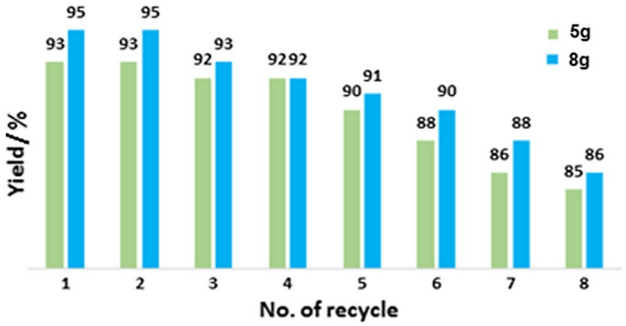

Fig. 6 Recycling of MCGC (1) in the synthesis of **5g** and **8g** as model substrates

General procedure for the synthesis of benzimidazoloquinazoline derivatives 5a–5h

A 10 cm^3 round-bottomed flask was charged with 2-aminobenzimidazole (**2**, 1 mmol), aromatic aldehyde (**3**, 2 mmol), dimedone (**4**, 1 mmol), MCGC (**1**, 15 mg), and 5 cm^3 ethanol and placed in an ultrasonic cleaner. The surface of water in the water bath of ultrasonic cleaner was slightly upper than the surface of reactants. After that, the reaction mixture was irradiated under the irradiation frequency of 25 kHz at 30–32 °C for the time mentioned in the Table 2. After completion of the reaction, as monitored by TLC (eluent *n*-hexane:ethyl acetate 1:3) the reaction was cooled down to room temperature, the catalyst **1** was separated using an external magnet and the residue was dried at room temperature to afford the crude product. Finally, the crude product was recrystallized from ethanol and water to obtain the pure product.

General procedure for the synthesis of 1,4-dihydropyridines derivatives 8a–8h'

A 10 cm^3 round-bottomed flask was filled with aromatic aldehyde (**3**, 1 mmol), ethyl acetoacetate (**6**, 2 mmol),

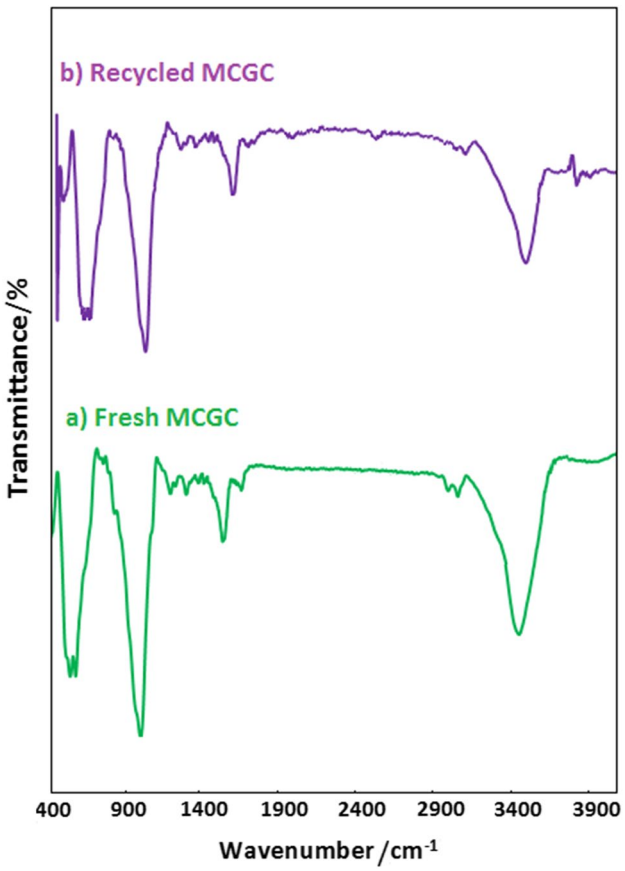

Fig. 7 FT-IR of fresh MCGC (**a**) and recycled MCGC (**b**) after run 8th

ammonium acetate (**7**, 1 mmol), MCGC (**1**, 15 mg), and 5cm^3 ethanol and placed in an ultrasonic cleaner. The level of water in the water bath of ultrasonic cleaner was slightly upper than the surface of reactants in the round-bottomed flask. The irradiation of reaction mixture was carried out under the irradiation frequency of 25 kHz at 40–42 °C for the appropriate time as indicated in the Table 2. The progress

of the reaction was monitored by TLC (eluent *n*-hexane:ethyl acetate 3:1). After completion of the reaction, the catalyst **1** was separated using an external magnet. Then, the catalyst **1** was collected by an external magnet and the residue was dried at room temperature to afford the crude product. Finally, after addition of 10 cm^3 ethanol to the reaction mixture, the desired product obtained by cooling in an ice-bath with high purity.

Acknowledgements We are thankful for the financial support from Chemical Injuries Research Center, Systems Biology and Poisonings Institute, Baqiyatallah University of Medical Sciences, Tehran, Iran.

References

1. Guin D, Baruwati B, Manorama SV (2007) Org Lett 9:1419
2. Sadeghzadeh SM (2016) Catal Lett 146:2555
3. Samoilova N, Krayukhina M, Naumkin A, Yamskov I (2018) Monatsh Chem 149:1179
4. Kasprzak A, Bystrzejewski M, Poplawska M (2018) Dalton Trans 47:6314
5. Anastas P, Eghbali N (2010) Chem Soc Rev 39:301
6. Pourjavadi A, Motamedi A, Hosseini SH, Nazari M (2016) RSC Adv 6:19128
7. Li D-D, Zhang J-W, Cai C (2018) Catal Commun 103:47
8. Dekamin MG, Azimoshan M, Ramezani L (2013) Green Chem 15:811
9. Shaabani A, Hezarkhani Z, Badali E (2015) RSC Adv 5:61759
10. Rao SN, Mohan DC, Adimurthy S (2014) Green Chem 16:4122
11. Shen C, Qiao J, Zhao L, Zheng K, Jin J, Zhang P (2017) Catal Commun 92:114
12. Lal J, Gupta SK, Agarwal DD (2012) Catal Commun 27:38
13. Zeng M, Zhang X, Shao L, Qi C, Zhang XM (2012) J Organomet Chem 704:29
14. Sudheesh N, Sharma SK, Shukla RS (2010) J Mol Catal A Chem 321:77
15. Kühbeck D, Saidulu G, Reddy KR, Díaz DD (2012) Green Chem 14:378
16. Abdelhamid IA (2009) Synlett 2009:625
17. Makhubela BC, Jardine A, Smith GS (2011) Appl Catal A 393:231
18. Bao Y, Shao L, Xing G, Qi C (2019) Int J Biol Macromol 130:203
19. Saikia G, Ahmed K, Gogoi SR, Sharma M, Talukdar H, Islam NS (2019) Polyhedron 159:192
20. Rangraz Y, Nemati F, Elhampour A (2018) Int J Biol Macromol 117:820
21. Chtchigrovsky M, Primo A, Gonzalez P, Molvinger K, Robitzer M, Quignard F, Taran F (2009) Angew Chem Int Ed 48:5916
22. Lee M, Chen B-Y, Den W (2015) Appl Sci 5:1272
23. Tap H, Sugimoto R (2018) Appl Surf Sci 434:188
24. Kumar S, Deepak V, Kumari M, Dutta P (2016) Int J Biol Macromol 84:349
25. Zhai X, Sun P, Luo Y, Ma C, Xu J, Liu W (2011) J Appl Polym Sci 121:3569
26. Maleki A, Firouzi-Haji R, Hajizadeh Z (2018) Int J Biol Macromol 116:320
27. Ramezanpour S, Panahi A, Rominger F (2018) Monatsh Chem 149:625
28. Palermo V, Sathicq ÁG, Constantieux T, Rodríguez J, Vázquez PG, Romanelli GP (2016) Catal Lett 146:1634
29. Neochoritis CG, Zhao T, Dömling A (2019) Chem Rev 119:1970
30. Dömling A (2006) Chem Rev 106:17
31. Kalinski C, Lemoine H, Schmidt J, Burdack C, Kolb J, Umkehrer M, Ross G (2008) Synthesis 2008:4007
32. Mamaghani M, Tabatabaeian K, Shirini F, Rassa M (2012) Bioorg Med Chem Lett 22:5956
33. Dandia A, Singh R, Bhaskaran S, Samant SD (2011) Green Chem 13:1852
34. Wu C, Lu L-H, Peng A-Z, Jia G-K, Peng C, Cao Z, Tang Z, He W-M, Xu X (2018) Green Chem 20:3683
35. Mason TJ (1997) Chem Soc Rev 26:443
36. O'Hagan D (2000) Nat Prod Rep 17:435
37. Alagarsamy V, Pathak US (2007) Bioorg Med Chem 15:3457
38. Alagarsamy V (2004) Pharmazie 59:753
39. Alagarsamy V, Murugananthan G, Venkateshperumal R (2003) Biol Pharm Bull 26:1711
40. Hour M-J, Huang L-J, Kuo S-C, Xia Y, Bastow K, Nakanishi Y, Hamel E, Lee K-H (2000) J Med Chem 43:4479
41. Alagarsamy V, Revathi R, Meena S, Ramaseshu K, Rajasekaran S, De Clerco E (2004) Indian J Pharm Sci 66:459
42. Smutny T, Nova A, Drechslerová M, Carazo A, Hyrsova L, Kunes J, Pour M, Špulák M, Pavek P (2016) J Med Chem 59:4601
43. Ahmad I (2017) MedChemComm 8:871
44. Tebbe MJ, Spitzer WA, Victor F, Miller SC, Lee CC, Sattelberg TR, McKinney E, Tang JC (1997) J Med Chem 40:3937
45. Charifson PS, Grillot AL, Grossman TH, Parsons JD, Badia M, Bellon S, Deininger DD, Drumm JE, Gross CH, LeTiran A (2008) J Med Chem 51:5243
46. White AW, Almassy R, Calvert AH, Curtin NJ, Griffin RJ, Hostomsky Z, Maegley K, Newell DR, Srinivasan S, Golding BT (2000) J Med Chem 43:4084
47. Naesdal J, Bodemar G, Walan A (1984) Scand J Gastroenterol 19:916
48. Kamali F, Shirini F (2017) New J Chem 41:11778
49. Sheldon R, Arends A, Hanefeld U (2007) Green chemistry and catalysis. Wiley, VCH Verlag GmbH and Co KgaA, Weinheim
50. Heravi MM, Derikvand F, Ranjbar L (2010) Synth Comm 40:677
51. Gajaganti S, Kumari S, Kumar D, Allam BK, Srivastava V, Singh S (2018) J Heterocycl Chem 55:2578
52. Boecker RH, Guengerich FP (1986) J Med Chem 29:1596
53. Sirisha K, Bikshapathi D, Achaiah G, Reddy VM (2011) Eur J Med Chem 46:1564
54. Klusa V (1995) Drugs Future 20:135
55. Bretzel RG, Bollen CC, Maeser E, Federlin KF (1993) Am J Kidney Dis 21:S53
56. Janis RA, Triggle D (1983) J Med Chem 26:775
57. Mager P, Coburn R, Solo A, Triggle D, Rothe H (1992) Drug Des Discov 8:273
58. Itoh T, Nagata K, Miyazaki M, Ishikawa H, Kurihara A, Ohsawa A (2004) Tetrahedron 60:6649
59. Dondoni A, Massi A, Minghini E, Bertolasi V (2004) Tetrahedron 60:2311
60. Cherkupally SR, Mekala R (2008) Chem Pharm Bull 56:1002
61. Safari J, Banitaba SH, Khalili SD (2011) J Mol Catal Chem 335:46
62. Albadi J, Shirini F, Ghabezi B, Seiadatnasab T (2017) Arab J Chem 10:S509
63. Dekamin MG, Kazemi E, Karimi Z, Mohammadalipoor M, Naimi-Jamal MR (2016) Int J Biol Macromol 93:767
64. Mahinpour R, Moradi L, Zahraei Z, Pahlevanzadeh N (2018) J Saudi Chem Soc 22:876
65. Kumar P, Kadyan K, Duhan M, Sindhu J, Hussain K, Lal S (2019) Chem Pap 73:1153
66. Davarpanah J, Ghahremani M, Najafi O (2019) J Mol Struct 1177:525
67. Rekunge DS, Khatri CK, Chaturbhuj GU (2017) Tetrahedron Lett 58:1240
68. Khaskel A, Barman P (2016) Heteroat Chem 27:114
69. Aftan MM (2018) Tikrit J Pure Sci 23:83
70. Hemmati B, Javanshir S, Dolatkhah Z (2016) RSC Adv 6:50431
71. Mousavi MR, Maghsoodlou MT (2015) J Iran Chem Soc 12:743

72. Yao C, Lei S, Wang C, Li T, Yu C, Wang X, Tu S (2010) J Heterocycl Chem 47:26
73. Weber L (2002) Drug Discov Today 7:143
74. Mousavi MR, Maghsoodlou MT (2014) Monatsh Chem 145:1967
75. Suslick KS, Hammerton DA, Cline RE (1986) J Am Chem Soc 108:5641
76. Tameh FA, Safaei-Ghomi J, Mahmoudi-Hashemi M, Shahbazi-Alavi H (2016) RSC Adv 6:74802
77. Maleki A, Rahimi J (2018) J Porous Mat 25:1789
78. Amoozadeh A, Rahmani S (2015) J Mol Catal A Chem 396:96